

# Position Tracking Control of Flexible Piezo-beam Considering Actuator Hysteresis 작동기 히스테리시스를 고려한 유연피에조빔의 위치추적제어

Phuong-Bac Nguyen\* and Seung-Bok Choi<sup>†</sup>

프엉박 · 최승복

**Key words:** Hysteresis (히스테리시스), Piezoceramic Actuator (압전작동기), Preisach Model (프라이작 모델), Position Tracking Control (위치추적제어).

## ABSTRACT

This paper presents a position tracking control of a flexible beam using the piezoelectric actuator. This is achieved by implementing both feedforward hysteretic compensator of the actuator and PID feedback controller. The Preisach model is adopted to develop the feedforward hysteretic compensator. In the design of the compensator, estimated displacement of the piezoceramic actuator is used on the basis of the limiting triangle database that results from collecting data of the main reversal curve and the first order ascending curves. Experimental implementation is conducted for position tracking control and performance comparison is made between a PID feedback controller without considering the effect of hysteresis, and a PID feedback controller integrated with the feedforward hysteretic compensator.

## 1. Introduction

As it is well known, a smart structure is a system included to smart materials to perform sensing, control, and actuation. Smart structures have outstanding characteristics such as high resolution and fast response. So, they are being applied increasingly in many fields such as micro-positioning [1-3], vibration suppression [4]. However, their high nonlinearity limits control accuracy as well as the scope of application. Hysteresis in piezoceramic materials is a kind of nonlinearity with nonlocal memory. Because of hysteresis, the response of the piezoceramic to an applied input voltage is impossible to predict without considering its effect. Therefore, in order to gain a high performance in control, the hysteresis has to be reduced or eliminated.

The main contribution of this work is to develop the compensator for hysteresis of the piezoactuator and incorporate with the flexible beam structure in order to achieve an accurate position tracking control of tip displacement. The hysteretic compensator is designed on the basis of Preisach model. In Preisach model, the main reversal curve and the first order ascending curves for numerical implementation are used to get limit triangle database. On the other hand, the flexible beam is modeled

using finite element method to obtain modal parameters such as natural frequency. Then, the position tracking control of a flexible piezoelectric beam is accomplished by using a PID feedback controller combined with the feedforward hysteretic compensator. Performance comparison between without and with the hysteretic compensator is made via experimental realization.

## 2. Modeling of Piezoactuator Hysteresis

The Preisach model can be numerically implemented by two approaches [5]; the first is to use the following formula for the computation of the input.

$$\mu(\alpha_1, \beta_1) = -\frac{\partial^2 Y(\alpha_1, \beta_1)}{\partial \alpha \partial \beta} \quad (1)$$

where,  $Y(\alpha_1, \beta_1)$  is the change in output  $y(t)$  as the input decreases from  $\alpha_1$  to  $\beta_1$ . Although this approach is straightforward, it encounters the main difficulty that the double numerical differentiation of experimentally obtained data may amplify errors seriously. Therefore, the second approach, the numerical implementation of the Preisach model, is preferable. It circumvents the above difficulty. This approach is based on the data collected from the main ascending curve and the first order reversal curves [5-7].

In our work, instead of using the data collected from the main curve and the first order reversal curves, we use the data collected from the main reversal curve and the first order ascending curves for numerical implementation of the Preisach model. For the case of monotonically

<sup>†</sup> 교신저자; 정회원, 인하대학교 기계공학과

E-mail: seungbok@inha.ac.kr

Tel: (032) 860-7319, Fax: (032) 868-1716

\* 인하대학교 대학원 기계공학과

increasing of excitation voltage, at the time  $t_n$ , the corresponding  $\alpha\beta$  plane is shown in the Figure 1.

The expansion of the piezoceramic can be expressed as follows.

$$y_{pre}(u(t_n)) = y_{ex}(m) + \iint_{\Delta S} \mu(\alpha, \beta) d\alpha d\beta \quad (2)$$

where,  $y_{ex}(m)$  is the expansion of the piezoceramic at the nearest pair of extrema (include one maximum and one minimum). We assume that there are three pairs of extrema  $(\alpha_i, \beta_i)$   $i = 1, 2, 3$ . Therefore,  $S^+(t_n)$  is subdivided into sub-regions as shown in Figure 2.

The expansion of the piezoceramic actuator is given as

$$y_{ex}(3) = H(S_3^+) + H(S_2^+) + H(S_1^+) \quad (3)$$

where, from the outputs corresponding regions  $S_i^+$  ( $i = 1, 2, 3$ ) shown in Figure 3, the following mathematical expressions can be obtained.

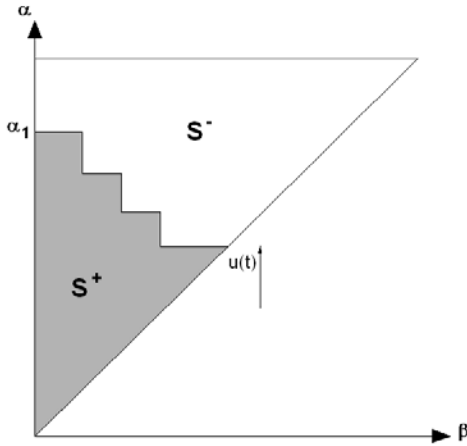


**Figure 1** The  $\alpha\beta$  plane in the case of monotonically increasing of excitation voltage

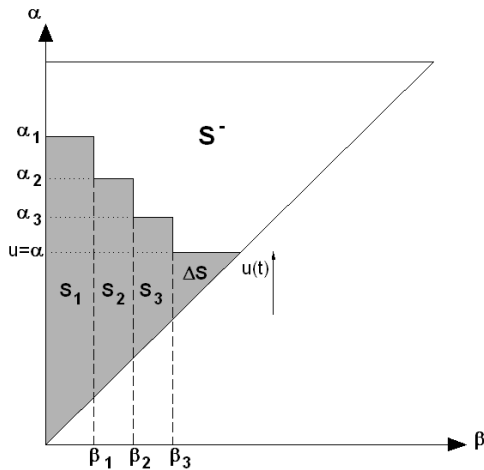


**Figure 2** The sub-regions constitute  $S^+$

$$H(S_3^+) = F(\beta_2, \alpha_3) - F(\beta_3, \alpha_3) \quad (4a)$$

$$H(S_2^+) = F(\beta_1, \alpha_2) - F(\beta_2, \alpha_2) \quad (4b)$$

$$H(S_1^+) = F(0, \alpha_1) - F(\beta_1, \alpha_1) \quad (4c)$$

where,  $F(\beta_j, \alpha_i)$  is the value corresponding to the triangle limited by  $\beta_j$  and  $\alpha_i$ . According to Figure 4, this value can be expressed as follows.

$$F(\beta_i, \alpha_j) = g(\beta_i, \alpha_j) - g(\beta_i) \quad (5)$$

where,  $g(\beta_i, \alpha_j)$  is the value at input  $\alpha_j$  of first order ascending curve  $\beta_i$ ;  $g(\beta_i)$  is the value at the input  $\beta_i$  of main reversal curve. Substituting Eqs. (4) and (5) into Eqs. (2) yields

$$y_{ex}(3) = g(\beta_3) + \sum_{k=1}^3 [g(\beta_{k-1}, \alpha_k) - g(\beta_k, \alpha_k)] \quad (6)$$

In general, with  $m$  pairs of extrema, one has the following form.

$$y_{ex}(m) = g(\beta_m) + \sum_{k=1}^m [g(\beta_{k-1}, \alpha_k) - g(\beta_k, \alpha_k)] \quad (7)$$

The second part of Eq. (2) is the value corresponding to the triangle limited by  $\beta_m$  and  $u(t_n)$  and expressed as follows.

$$\begin{aligned} \iint_{\Delta S} \mu(\alpha, \beta) d\alpha d\beta &= F(\beta_m, u(t_n)) \\ &= g(\beta_m, u(t_n)) - g(\beta_m) \end{aligned} \quad (8)$$

Substituting Eqs. (7) and (8) into Eq. (2) yields

$$y_{pre}(u(t_n)) = g(\beta_m, u(t_n)) + \sum_{k=1}^m [g(\beta_{k-1}, \alpha_k) - g(\beta_k, \alpha_k)] \quad (9)$$

Similarly, for the case of monotonically decreasing of excitation voltage as shown in Figure 5, an expression for expansion of piezoceramic actuator is developed as

$$\begin{aligned} y_{pre}(u(t_n)) &= g(\beta_2, \alpha_3) - g(u(t_n), \alpha_3) \\ &+ \sum_{k=1}^2 [g(\beta_{k-1}, \alpha_k) - g(\beta_k, \alpha_k)] \end{aligned} \quad (10)$$

In general, with  $m$  pairs of extrema, we have the following form.

$$\begin{aligned} y_{pre}(u(t_n)) &= g(\beta_{m-1}, \alpha_m) - g(u(t_n), \alpha_m) \\ &+ \sum_{k=1}^{m-1} [g(\beta_{k-1}, \alpha_k) - g(\beta_k, \alpha_k)] \end{aligned} \quad (11)$$

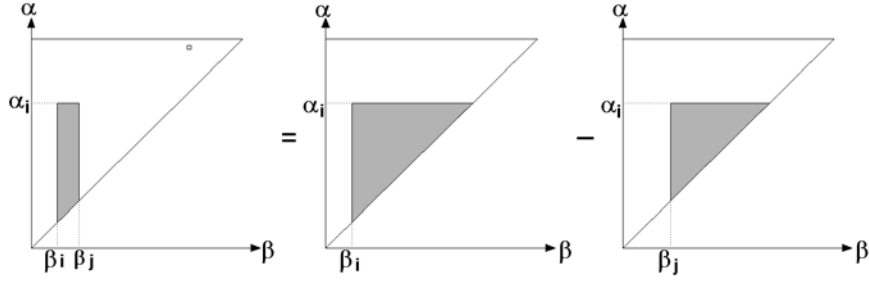


**Figure 3** The geometric calculation of  $H(S_i^+)$

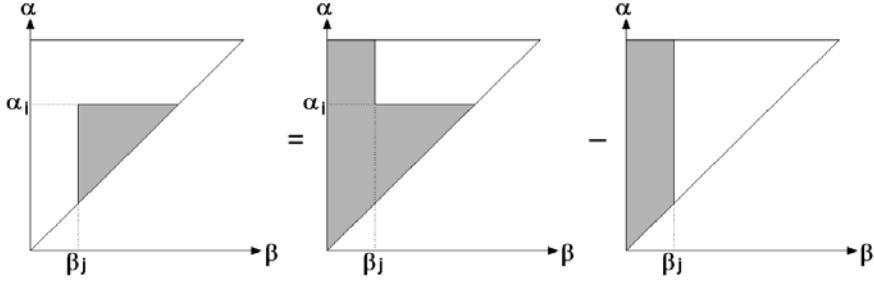


**Figure 4** The geometric calculation of  $F(\beta_i, \alpha_j)$

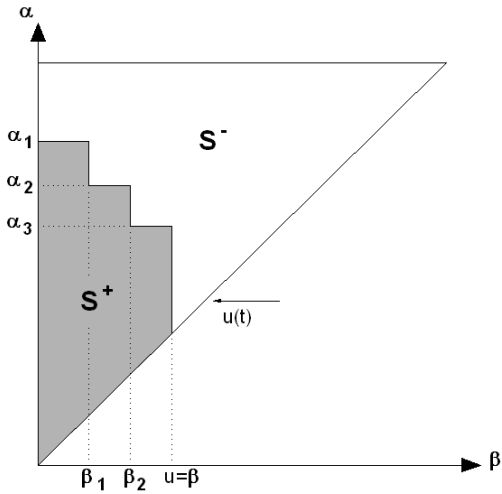


**Figure 5** The  $\alpha\beta$  plane in the case of monotonically decreasing of excitation voltage

Eqs. (9) and (11) give a numerical approach of Preisach model. In order to implement the model equation to determine the output to the input, a series of first-order reversal functions and a main ascending function for the piezoceramic actuator that are measured under static condition (i.e. the frequency of excitation voltage is fixed and set to be low) must be experimentally determined in advance. In our work, we use a series of first-order ascending functions  $g(\beta, \alpha)$  and a main reversal function  $g(\beta)$  for the experiment database. In the case the point  $(\beta, \alpha)$  does not lie on the grid point, it is determined by linear interpolation as follows.

$$g(\beta, \alpha) = c_0^{\beta\alpha} + c_1^{\beta\alpha} \beta + c_2^{\beta\alpha} \alpha + c_3^{\beta\alpha} \alpha\beta \quad (12)$$

Or

$$g(\beta, \alpha) = c_0^{\beta\alpha} + c_1^{\beta\alpha} \beta + c_2^{\beta\alpha} \alpha \quad (13)$$

Eq. (12) is used in the case the point  $(\beta, \alpha)$  lies in a rectangle element, otherwise in the case the point  $(\beta, \alpha)$  lies in a triangle element, Eq. (13) is used.

### 3. Design of Hysteretic Compensator

For the case of monotonically increasing of expansion  $y_d(t_n) > y_d(t_{n-1})$ , Eq. (9) can be written as

$$y_d(t_n) = g(\beta_m, v(t_n))$$

$$+ \sum_{k=1}^m [g(\beta_{k-1}, \alpha_k) - g(\beta_k, \alpha_k)] \quad (14)$$

Substituting Eq. (12) into Eq. (14) yields

$$y_d(t_n) = c_0^{\beta_m v(t_n)} + c_1^{\beta_m v(t_n)} \beta_m + [c_2^{\beta_m v(t_n)} + c_3^{\beta_m v(t_n)} \beta_m] v(t_n) + \sum_{k=1}^m [g(\beta_{k-1}, \alpha_k) - g(\beta_k, \alpha_k)] \quad (15)$$

Therefore, the expression for estimating  $v(t_n)$  is obtained by

$$v(t_n) = \frac{y_d(t_n) - [c_0^{\beta_m v(t_n)} + c_1^{\beta_m v(t_n)} \beta_m] - \sum_{k=1}^m [g(\beta_{k-1}, \alpha_k) - g(\beta_k, \alpha_k)]}{[c_2^{\beta_m v(t_n)} + c_3^{\beta_m v(t_n)} \beta_m]} \quad (16)$$

Similarly, for the case of monotonically decreasing of expansion  $y_d(t_n) < y_d(t_{n-1})$ , the expression for estimating  $v(t_n)$  is obtained by

$$v(t_n) = \frac{g(\beta_{m-1}, \alpha_m) - y_d(t_n) - c_0^{v(t_n)\alpha_m} - c_1^{v(t_n)\alpha_m} \alpha_m + \sum_{k=1}^{m-1} [g(\beta_{k-1}, \alpha_k) - g(\beta_k, \alpha_k)]}{[c_2^{v(t_n)\alpha_m} + c_3^{v(t_n)\alpha_m} \alpha_m]} \quad (17)$$

#### 4. Modeling of Flexible Beam

The schematic diagram of a composite beam is illustrated in Figure 6. This beam consists of an aluminum beam bonded by a piezoceramic actuator on one side of surface. In this section, the mathematical modeling of beam based on Euler-Bernoulli beam theory and finite element method is adopted.

The element stiffness matrix can be derived as

$$\mathbf{K}_e = \frac{EI}{l^3} \begin{bmatrix} 12 & 6l & -12 & 6l \\ 6l & 4l^2 & -6l & 2l^2 \\ -12 & -6l & 12 & -6l \\ 6l & 2l^2 & -6l & 4l^2 \end{bmatrix} \quad (18)$$

The element mass matrix can be derived as

$$\mathbf{M}_e = \frac{ml}{420} \begin{bmatrix} 156 & 22l & 54 & -13l \\ 22l & 4l^2 & 13l & -3l^2 \\ 54 & 13l & 156 & -22l \\ -13l & -3l^2 & -22l & 4l^2 \end{bmatrix} \quad (19)$$

The mass and stiffness matrices of entire beam are obtained by assembling the local mass and stiffness matrices using finite element method and combining the boundary conditions [8]. The governing equation of the beam in discretized form is given by

$$\mathbf{M}\ddot{\mathbf{Y}} + \mathbf{K}\mathbf{Y} = \mathbf{F}(t) \quad (20)$$

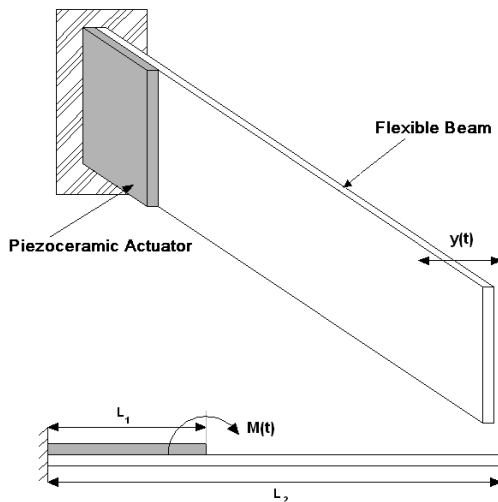


**Figure 6** The schematic diagram of the proposed flexible beam

where,  $\mathbf{Y}$  is the node displacement vector of the beam.  $\mathbf{M}$  and  $\mathbf{K}$  are respectively global mass and stiffness matrices.  $\mathbf{F}(t)$  is the node force vector acting on the beam.

The dynamic response of Eq. (20) can be expressed as

$$\mathbf{Y}(t) = \sum_{r=1}^N \boldsymbol{\phi}_r q_r(t) = \boldsymbol{\Phi} \mathbf{q}(t) \quad (21)$$

where,  $\boldsymbol{\phi}_r$  and  $\mathbf{q}(t)$  are respectively the natural mode shape and generalized coordinate vectors.

Substituting Eq. (21) into Eq. (20) and pre-multiplying by  $\boldsymbol{\phi}_i^T$  give the following.

$$M_i \ddot{q}_i(t) + K_i q_i(t) = f_i(t) \quad (22)$$

where,  $M_i = \boldsymbol{\phi}_i^T \mathbf{M} \boldsymbol{\phi}_i$ ;  $K_i = \boldsymbol{\phi}_i^T \mathbf{K} \boldsymbol{\phi}_i$ ;  $f_i(t) = \boldsymbol{\phi}_i^T \mathbf{F}(t)$

Dividing by  $M_i$  and adding the damping term  $2\xi_i \omega_i \dot{q}_i(t)$ , Eq. (22) can be written as

$$\ddot{q}_i(t) + 2\xi_i \omega_i \dot{q}_i(t) + \omega_i^2 q_i(t) = \frac{f_i(t)}{M_i} \quad (23)$$

For simplicity, the first mode of vibration is only considered in this work. From (23), the first mode of vibration equation can be expressed as

$$\ddot{q}(t) + 2\xi \omega \dot{q}(t) + \omega^2 q(t) = \frac{f_1(t)}{M_1} \quad (24)$$

#### 5. Experimental Results and Discussion

##### PID tracking control without feedforward hysteretic compensator

In this approach, the relationship between moment of the piezoceramic actuator and the voltage is considered to be linear [9].

$$M_p(t) = c \cdot v(t) \quad (25)$$

where,  $c$  is the nominal (known) constant and dependent on material and geometrical properties of the beam. A discrete time PID controller can be expressed as follows [10].

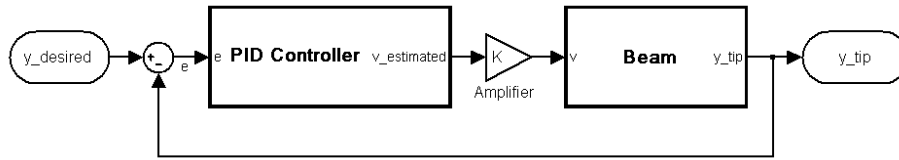


**Figure 7** The diagram block for discrete time PID tracking control without considering hysteretic behavior

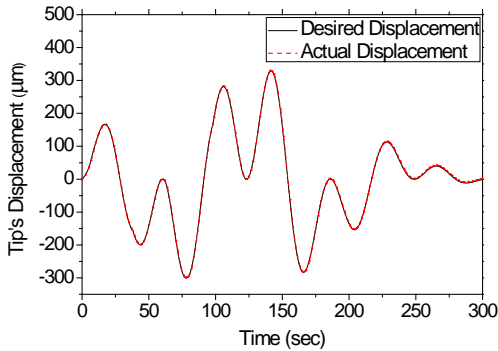


**Figure 8** Arbitrary waveform displacement at the tip of the beam for discrete time PID tracking control without considering hysteretic behavior

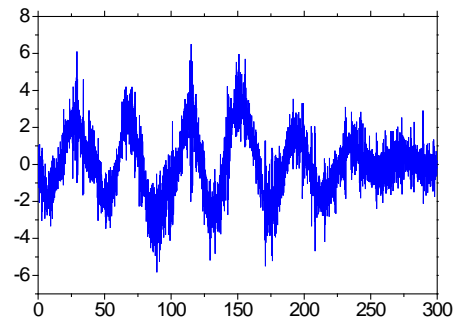


**Figure 9** The error curve between desired and actual arbitrary waveform for discrete time PID tracking control without considering hysteretic behavior

$$v(k) = K_p \left\{ e(k) + \frac{T}{T_I} \sum e(k) + \frac{T_D}{T} [e(k) - e(k-1)] \right\} \quad (26)$$

The diagram block for discrete time PID tracking control without considering hysteretic behavior is shown in Figure 7.

Figure 8 and Figure 9 show the tracking control response and tracking error curves respectively with an arbitrary desired displacement. The nonlinearity of piezoceramic actuator still limits the accuracy of PID controller. In theory, a linear controller cannot eliminate completely the error of a nonlinear system. The average error is 1.405  $\mu\text{m}$ .

#### PID tracking control with feedforward hysteretic compensator

In this control approach, the nonlinearity, hysteresis, is compensated separately. PID controller is then used to control the compensated system. The block diagram for discrete time PID tracking control with feedforward hysteretic compensator is shown in Figure 10. Figure 11 and Figure 12 show the tracking control response and tracking error curves respectively with an arbitrary waveform input signal. The average error is 0.649  $\mu\text{m}$ . As expected, the closed-loop PID tracking controller with the feedforward hysteretic compensator shows the smaller tracking error compared to the previous case.

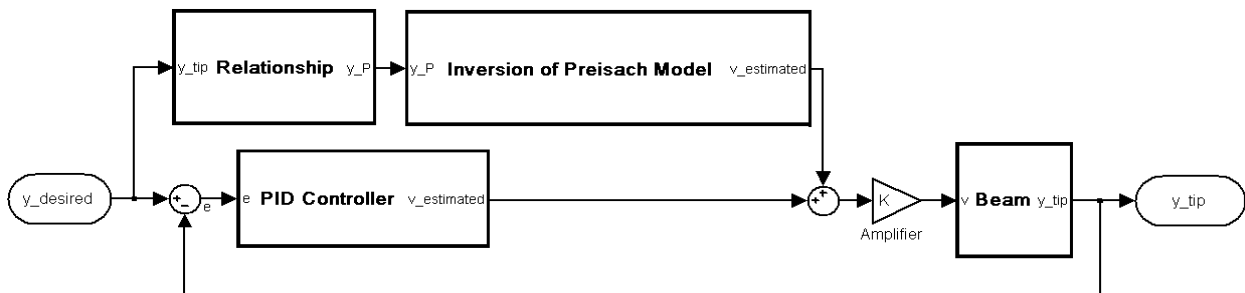


**Figure 10** The diagram block for discrete time PID tracking control with the feedforward hysteretic compensator

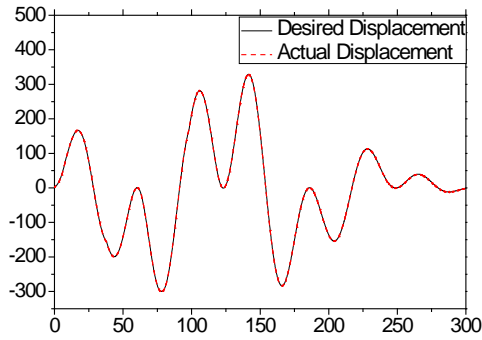


**Figure 11** Arbitrary waveform displacement at the tip of the beam for discrete time PID tracking control with the feedforward hysteretic compensator

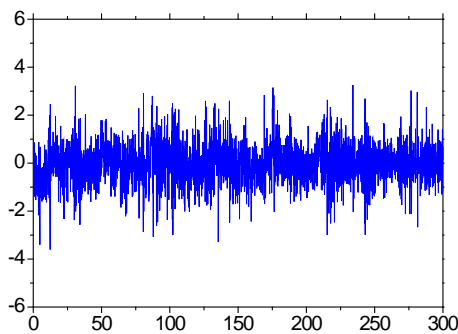


**Figure 12** The error curve between desired and actual arbitrary waveform for discrete time PID tracking control with the feedforward hysteretic compensator

## 6. Conclusion

In this work, the position tracking control system of a flexible beam considering hysteresis behavior was conducted. In the system modeling, the flexible beam was modeled by finite element method and Preisach model was used for hysteretic compensator. To implement the Preisach model, a set of first-order hysteretic ascending curves was measured. Higher order ascending curves were predicted based on experimental data and its effectiveness was experimentally verified. In order to increase the accuracy of control system, a PID were used for feedback controller. For experiment, two control approaches were proposed and implemented. They are PID tracking control without hysteretic behavior and PID tracking control with the feedforward hysteretic compensator. It has been demonstrated through experimental implementation that PID tracking control with the feedforward hysteretic compensator has the

better time and frequency tracking characteristics. It is finally remarked that in the near future the proposed control technique will be applied to more complicated systems such as position tracking control of dual servo stage system.

## Acknowledgement

This work was supported by the Ministry of Knowledge Economy (MKE) and Korea Industrial Technology Foundation (KOTEF) through the Human Resource Training Project for Strategic Technology.

## References

- (1) Katsushi Furutani, Mitsunori Urushibata and Naotake Mohri, "Displacement control of piezoelectric element by feedback of induced charge", *Nanotechnology* Vol. 9(2), (1998) 93-98.
- (2) Jing-Chung Shen, Wen-Yuh Jywe, Huan-Keng Chiang, Yu-Ling Shu, "Precision tracking control of a piezoelectric-actuated system", *Precision Engineering* Vol. 32(2), (2008) 71-78.
- (3) Ge P., Jouaneh M., "Tracking control of a piezoceramic actuator", *IEEE Transactions on Control Systems Technology* Vol. 4(3), (1996) 209-216.
- (4) Choi S.B. and Cheong C.C., "Vibration control of a flexible beam using SMA actuators", *Journal of Guidance, Control, and Dynamics* Vol. 19(5), (1996) 1178-1180.
- (5) I. Mayergoyz, "Mathematical models of hysteresis", New York: Springer-Verlag, 1991.
- (6) Ge P. and Jouaneh M., "Modeling hysteresis in piezoceramic actuators," *Precision Engineering*, vol. 17, (1995) 211-221.
- (7) Hu H., Mrad R. Ben, "A discrete-time compensation algorithm for hysteresis in piezoceramic actuators", *Mechanical Systems and Signal Processing* Vol. 18(1), (2004) 169-185.
- (8) Seshu P., "Textbook of Finite Element Analysis", 1st ed. Prentice Hall of India, New Delhi, (2004).
- (9) Baily T. and Hubbard J. E., "Distributed piezoelectric polymer active vibration control of a cantilever beam", *Journal of Guidance, Dynamics and Control*, Vol. 8(5), (1985) 605-611.
- (10) Franklin G.F., Powell J.D., and Workman M.L., "Digital Control of Dynamic Systems", Addison-Wesley, Reading, MA, (1992).